

White Blood Cell Counting Device for Dairy Cattle Using Microchannel Incorporating Light Scattering

Masaki Yamaguchi,^{1*} Tsuyoshi Nakamura,² and Hideki Sanjo³

¹Graduate School of Medicine, Science & Technology, Shinshu University,
3-15-1 Tokida, Ueda, Nagano 386-8567, Japan

²Research & Development Department, Citizen Finedevice Co., Ltd.,
4107-5 Miyota, Miyota-machi, Kitasaku-gun, Nagano 389-0925, Japan

³Department of Molecular and Cellular Immunology, Shinshu University School of Medicine,
3-1-1 Asahi, Matsumoto, Nagano 390-8621, Japan

(Received August 22, 2022; accepted October 28, 2022)

Keywords: microchannel, light scattering, field-flow fractionation, white blood cell, dairy cattle, raw bovine milk

White blood cell (WBC) count will greatly facilitate the timely diagnosis and management of health conditions of dairy cattle, including clinical mastitis. We propose a WBC counting device for dairy cattle using a microchannel with field-flow fractionation incorporating light scattering, which allows both the separation and counting of WBCs. The performance characteristics of the microchannel were optimized to separate particles by size through three-dimensional (3D) numerical simulations. The fabricated microchannel was evaluated using three mock beads with sizes of 3.5 μm representing milk fat globules (MFGs), 10 μm for WBCs, and 30 μm for cancer cells. The pinched flow microfluidic device was useful for separating particles with diameters of 10 and 30 μm . The WBC count was determined using the fabricated WBC counting device. Light scattering was effective for separating cells of 10 μm diameter or less such as MFGs and WBCs that pass through a close streamline. The linear regression analysis of the calibration curve for the WBC counting device showed a multiple determination coefficient of 0.98. The performance of our WBC counting device approached that of laboratory-based tests, allowing the quantitative and rapid analysis of the concentration of WBCs in raw bovine milk in field applications.

1. Introduction

The separation of particles in a size-dependent manner is essential for the determination of components in air and liquids. Particle counting is widely used in various field-based applications such as biochemical analyses and environmental assays, as well as in manufacturing industries and biomedical applications.⁽¹⁾ The somatic cell count in blood is an important indicator of health status and can be a marker of diseases such as cancer,^(2,3) ischemic heart disease,⁽⁴⁾ and mastitis.⁽⁵⁾ A technique of isolating white blood cells (WBCs) from red blood cells

*Corresponding author: e-mail: masakiy@shinshu-u.ac.jp
<https://doi.org/10.18494/SAM4090>

has been reported.⁽⁶⁾ Furthermore, the somatic cell count could be useful for testing livestock, as infection by bacteria and stress from milking devices cause dairy cattle mastitis.⁽⁷⁾

Field-flow fractionation (FFF) is one of the most versatile families of separation techniques used for fluid particles found in both air and liquids.^(8,9) FFF has numerous variants in terms of field type, instrument configuration, channel structure, and experimental conditions.⁽¹⁰⁾ It can be adopted to separate and characterize a variety of macromolecular and particulate materials, thus allowing them to be used for liquid chromatography and capillary electrophoresis. Since the introduction of a method of fabricating polydimethylsiloxane (PDMS) microchannels utilizing microfluidics proposed by Whitesides *et al.* in the late 1990s, the range of field-based applications of FFF has increased.⁽¹¹⁾ An early method used to separate particles by size was flow FFF using pillar-shaped periodic structures in a microchannel.⁽¹²⁾ A simplified structure utilizing asymmetrical flow FFF was proposed by Yamada and coworkers, which was named pinched flow fractionation.^(13,14)

However, some problems have remained in applying FFF to the diagnosis of dairy cattle mastitis. The dairy cattle mastitis can be estimated by monitoring concentrations of WBCs.⁽¹⁵⁾ Raw bovine milk includes different types of cells such as WBCs and cancer cells, whose mean diameters are 10 and <10 μm , respectively.^(16,17) Additionally, raw bovine milk from dairy cattle contains milk fat globules (MFGs). The diameter range of MFGs has been reported to be 0.2–15 μm ,⁽¹⁸⁾ 2.5–5.7 μm ,⁽¹⁹⁾ and 2.70–5.69 μm .⁽²⁰⁾ Thus, the development of a WBC counting device for dairy cattle requires the separation of WBCs and MFGs. Moreover, the monitoring of individual dairy cattle is required to identify which dairy cattle is affected by mastitis. It is necessary to test each dairy cattle using a portable device or to install a sensor for each milking machine. Thus, the WBC counting device requires the development of corresponding bioanalytical technologies that enable the rapid analysis and reporting of results using a portable device. Immediate access to dairy cattle would empower livestock workers to make timely and appropriate decisions for the testing of livestock in the field. However, no portable counting device that can separate WBCs from other particles contained in raw bovine milk from dairy cattle while simultaneously determining the concentration of WBCs has been proposed. Although a charge-coupled device (CCD) camera has been used for cell counting, it is not adoptable as a portable device.

To overcome these limitations, we focused on the use of a microchannel with light scattering as a particle counting method. Light scattering with high sensitivity using a miniaturized device can be achieved^(21–23) and has also been applied as a portable direct-reading instrument to measure PM_{2.5} in the atmosphere.⁽²⁴⁾ However, there have been limited calibration studies on cell counting instruments *in vivo*.

We designed a miniaturized WBC counting device that integrated a microchannel and light scattering and achieved particle separation and counting that is suitable for the evaluation of raw bovine milk from dairy cattle. The designed device consisted of a microchannel using PDMS, was based on pinched flow fractionation, and was equipped with an optical unit responsible for light scattering. We optimized the flow through the microchannel for pinched flow fractionation and evaluated its effect on separating particles by size. Subsequently, we evaluated the characteristics of separation and counting using both polymer mock microbeads and WBCs. Finally, we investigated the utility of the counting device to count WBCs using raw bovine milk from dairy cattle.

2. Materials and Methods

2.1 Chemicals

PDMS (KER-4690-A/BShin-Etsu Chemical Co., Ltd., Tokyo, Japan) was used for fabricating a microchannel. Polymer microbeads (1.05 of specific gravity) with three different diameters were prepared: 3.5 μm (SX-350H, polystyrene, Soken Chemical and Engineering Co., Ltd., Tokyo, Japan) and 10 and 30 μm (Nos. 72986 and 84135, polystyrene, Sigma-Aldrich, MO, USA). Glycerin (Cas no. 56-81-5, Kanto Chemical Co., Ltd., Tokyo, Japan) and a surfactant (Tween 20, Cas no. 9005-64-5, Sigma-Aldrich Co. LLC, MO, USA) were used to synthesize a sample liquid.

A murine lymphoma-derived cell line (YAC-1 lymphoma cell, Department of Microbiology, Faculty of Dentistry, Tohoku University, Japan) was obtained as WBCs.⁽²⁵⁾ To prevent bacterial contamination, 1% Penicillin-Streptomycin-Glutamine (10378016, Gibco, Carlsbad, CA, USA) was added to the sample liquid containing WBCs and to raw bovine milk samples. The WBCs were grown in RPMI-1640 culture medium (R8758, Sigma-Aldrich Inc., Darmstadt, Germany) supplemented with 10% heat-inactivated fetal bovine serum (FB-1365, Biosera Europe, Nuaille, France), 1% Penicillin-Streptomycin-Glutamine, and 50 μM 2-mercaptoethanol (Cas no. 60-24-2, MP Biomedicals, Irvine, CA, USA).⁽²⁶⁾ A cell viability imaging kit (R37610, ReadyProbes, Thermo Fisher Scientific K.K., Tokyo, Japan) was used to estimate the presence of cells.

2.2 Principle of WBC counting device

The schematic of the WBC counting device is presented in Fig. 1, which includes (i) two syringe pumps (Legato 100, KD Scientific Inc., MA, USA), (ii) a microchannel, and (iii) an optical unit. The microchannel has two inlets (Nos. 10000064 and 10000701, Microfluidic ChipShop GmbH, Jena, Germany): one is used for liquids with particles (sample liquid) and the other is used for liquids without particles (sheath liquid). The diameter, focal length, and irradiation angle of the lens used for the optical unit were 8 mm, $f = 11$ mm, and 40° , respectively, and two lenses with the same specifications were used.

Firstly, the sample and sheath liquids are continuously introduced into the microchannel from each inlet. The microchannel also features a pinched segment followed by a broadened segment. The particles are focused on one sidewall in the pinched segment by controlling the flow rates from both inlets. Then, the particles align with the sidewall regardless of their size. At the boundary between the two segments, a force toward the outflow side of the microchannel (x -axis) is exerted mainly on large particles by the spreading flow profile, whereas a force toward the sidewall of the broadened segment (y -axis) is exerted mainly on small particles. Thus, the particles are separated perpendicularly to the y -axis direction according to their sizes.

The setup of a fabricated optical unit based on light scattering to determine the concentration of WBCs is shown in Fig. 1(b). A laser diode (LD; L12170, radiant flux of 1200 mW, wavelength of 870 nm, Hamamatsu Photonics K.K., Hamamatsu, Japan) was used as the light source and a photodiode (S7610-10, Hamamatsu Photonics K.K.) was used as a detector for light scattered at

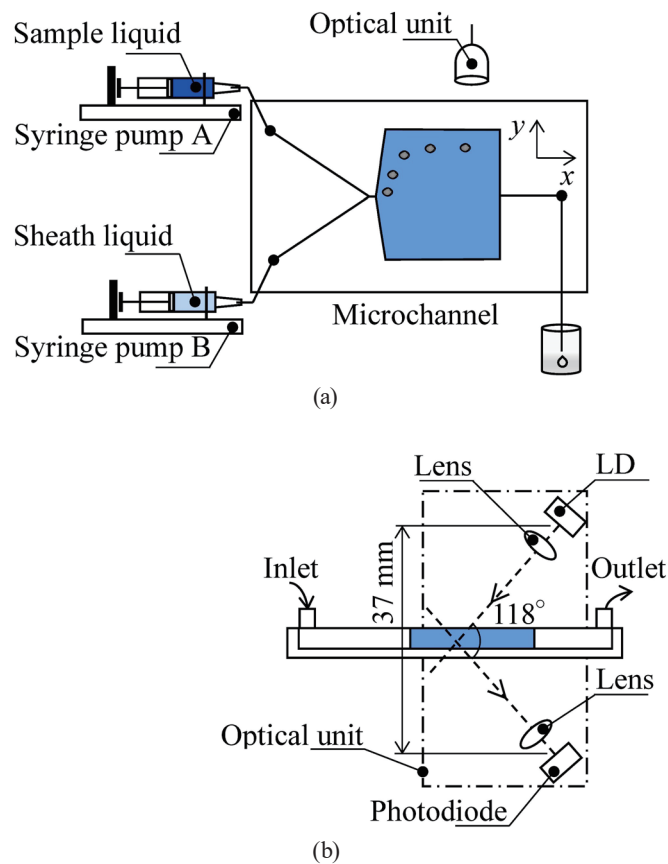


Fig. 1. (Color online) Schematic of WBC counting device using microchannel incorporating light scattering (LD: laser diode): (a) top and (b) side views.

an angle of 118° (the angles of incidence and reflection to the target were set to the same value of 31°).

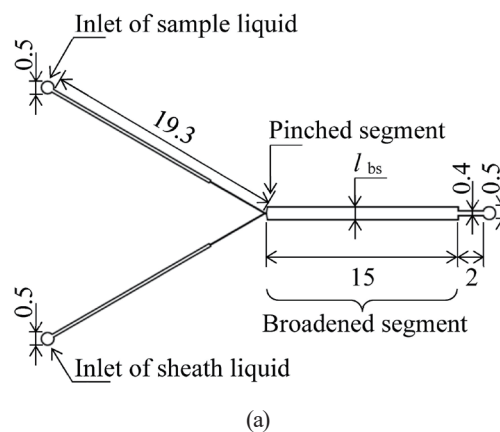
2.3 Design and fabrication of microchannel

The microchannel used for the WBC counting device was designed by 3D numerical simulation using thermo-fluid software (scSTREAM Ver.13, Software Cradle Co., Ltd., Japan) based on the continuum surface force model using the finite volume method. An orthogonal grid was used for the 3D computational fluid dynamics. The thermo-fluid software was operated on a parallel computer with 16 degrees of parallelism. A workstation (Precision T7810, CPU: Dual Intel® Xeon processor E5-2667 × 2 systems, 3.2 GHz, OS: Windows 7, HPC Solutions, Inc., Japan) was used for the calculations. A multi-interface advection and reconstruction solver was used for interface capture,⁽²⁷⁾ and a first-order upwind difference scheme was used for calculating the convection term.^(28,29) The second-order central difference approximation was used for calculating the viscosity term, and a semi-implicit method for pressure-linked equations was used to calculate the pressure gradient. In this research, the flow rate was defined by the

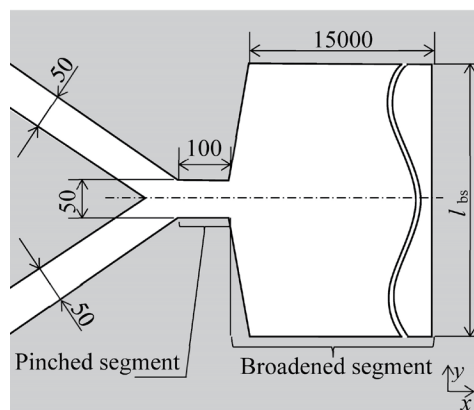
sample liquid:sheath liquid ratio. The positions of the sample liquid in the pinched segment (y_{ps}) and broadened segment (y_{bs}) were calculated from the flow rate and the width of the broadened segment (l_{bs}), which were used as parameters.

Figure 2 shows the architecture of the microchannel with the pinched and broadened segments. The 3D mesh model shown in Fig. 2(b) has 7515000 elements and 7844252 nodes. The density, viscosity, and surface tension of water were set to 998.2 kg/m^3 , $1.016 \text{ mPa}\cdot\text{s}$, and 72.7 mN/m , respectively. The streamlines were calculated with the flow rate (sample liquid:sheath liquid ratio) and the width of the broadened microchannel segment, l_{bs} , as variables.

A master mold of the microchannel was fabricated by using a lithography-based approach. A wafer was coated with a negative photoresist (THB111N, Tokyo JSR Co., Tokyo, Japan) using a spin coater (1HDXII, Mikasa Co., Tokyo, Japan). The thickness of the photoresist was set to $7 \text{ }\mu\text{m}$. The photoresist was exposed to a pattern using a layout mask and a mask aligner (UX-1000, Ushio Inc., Tokyo, Japan). Deep reactive ion etching (DRIE) was performed for 14 min using a Si DRIE system (MUC-21, SPP Technologies Co., Ltd., Tokyo, Japan). The photoresist was then removed using acetone. Finally, the microchannel was fabricated by replica modeling using PDMS.⁽¹¹⁾



(a)



(b)

Fig. 2. Architecture of the microchannel with the pinched and broadened segments (the groove depth of the microchannel was unified to $50 \text{ }\mu\text{m}$): (a) fabricated and (b) simulation models (units in μm).

2.4 Separation of mock microbeads

The separation characteristics of a fabricated microchannel were evaluated using polymer microbeads with three different diameters as a mock test. The 3.5 μm polymer microbeads were used as MFGs (mock microbeads 3.5 μm) because the mean diameter of MFGs has been estimated to be this value.^(18–20) The 10 and 30 μm polymer microbeads were used as WBCs (mock microbeads 10 μm) and cancer cells (mock microbeads 30 μm).^(16,17) Samples of both the sample and sheath liquids were prepared using distilled water with glycerin and a surfactant. Glycerin was added to match the specific gravity of polystyrene (1.05) to prevent particle settling. The surfactant was added in order to prevent the agglomeration of polymer beads. Two different flow rates were compared: 1:10 (sample and sheath liquids were 0.2 and 2 $\mu\text{L}/\text{min}$, respectively) and 1:20 (0.1 and 2 $\mu\text{L}/\text{min}$). The separation of the microbeads was observed by using a CCD camera (VHX-2000, Keyence Co., Osaka, Japan) and a lens (2 million pixels, VH-Z150, Keyence Co.). The number of particles was measured at $x = 1,000 \mu\text{m}$. The results were shown as means \pm standard deviation (SD).

2.5 Separation of WBCs

Cells separation and counting were performed using the YAC-1 cell line as WBCs. Prior to use, the cells were diluted to a concentration of 3.3×10^3 cells/ μL and used as the sample liquid containing WBCs.

Firstly, the separation performance of the WBCs by the microchannel was measured by using the CCD camera. Next, the detected signals for 3.5 and 10 μm mock beads, and WBCs were compared by using the WBC counting device. Hereafter, the flow rate was set at 1:10 on the basis of the calculated and measured results.

2.6 Counting of WBCs in raw bovine milk

Finally, cells in raw bovine milk were counted using the WBC counting device. The raw bovine milk was collected from a Holstein-Friesian cow at a cooperating dairy farm of Shinshu University (latitude 35°51'S, longitude 137°56'E). Penicillin-Streptomycin-Glutamine was added to the raw bovine milk, which was cooled to 4 °C on ice during transportation to the laboratory. A disposable cell counting plate (CP-BT, Burkert-Turk type, Ina-Optika Co., Osaka, Japan) was used to identify the number of MFGs. A cell viability imaging kit and an inverted phase contrast microscope (IX-71, Olympus Co., Tokyo, Japan) were used to identify the presence of WBCs in raw bovine milk and to count them. The number of output signals per minute was measured when the concentration of WBCs in the raw milk was changed by dilution. To draw a calibration curve between the number of output signals and the concentration of WBCs for the WBC counting device, the raw bovine milk was diluted serially to a concentration of 0.1 to 0.01.

3. Results

3.1 Design and fabrication of WBC counting device

The streamlines were calculated for each condition [Fig. 3(a)]. The lower position of the streamline for the sample liquid from the center at the pinched segment, y_{ps} , increased proportionally to the flow rate [Fig. 3(b)]. y_{ps} was determined to be 17.3 and 19.8 μm for flow rates of 1:10 and 1:20, respectively. The width of the streamline for the sample liquid from the center of the broadened segment, y_{bs} , increased proportionally to the flow rate [Fig. 3(c)]. The positions of the particles reaching the broadened segments were calculated for each particle size according to the streamline passing through the pinched segment [Fig. 3(d)].

3.2 Separation of mock microbeads

For the flow rate of 1:10, the positions in the broadened segment for 3.5, 10, and 30 μm mock microbeads were in the ranges of 406.3–496.3 μm ($456.6 \pm 21.8 \mu\text{m}$), 412.6–482.5 μm ($456.9 \pm 16.5 \mu\text{m}$), and 273.9–371.3 μm ($343.1 \pm 13.7 \mu\text{m}$), respectively [Fig. 4(a)]. The coefficients of variation (CVs) of y_{bs} for 3.5, 10, and 30 μm mock microbeads were 4.7, 3.6, and 4.0%, respectively. For the flow rate of 1:20, the positions in the broadened segment for 3.5, 10, and 30 μm mock microbeads were in the ranges of 417.2–482.5 μm ($453.9 \pm 16.4 \mu\text{m}$), 395.9–463.1 μm

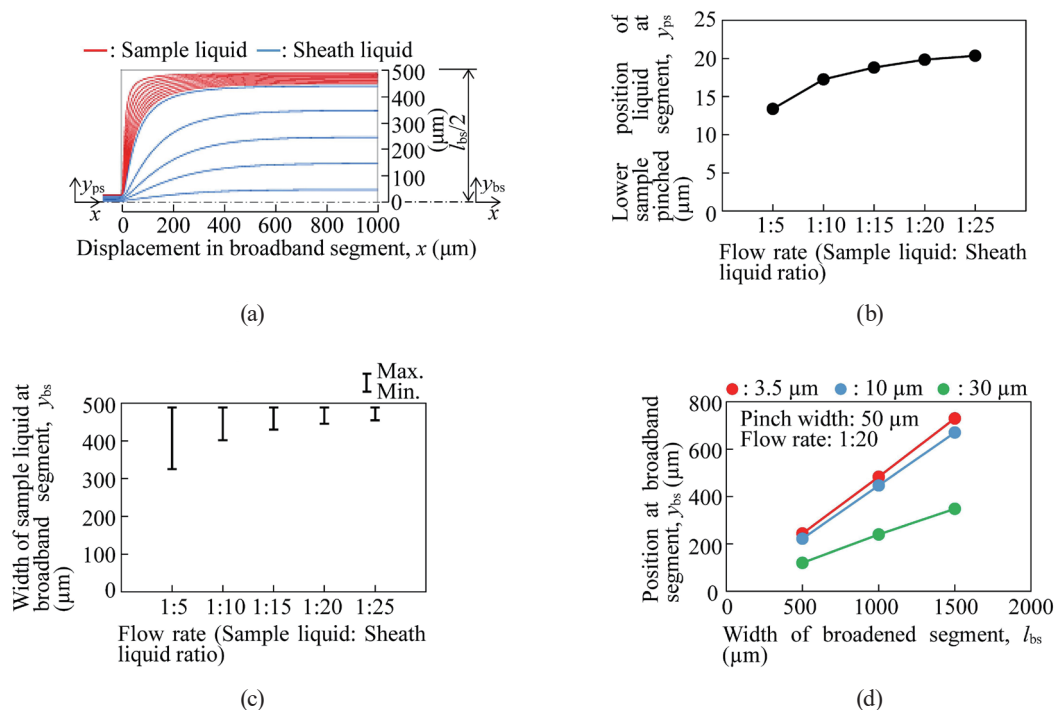


Fig. 3. (Color online) Calculated results of streamline for sample liquid in microfluidic device (units in μm): (a) streamline (flow rate = 1:20), (b) lower position at pinched segment, (c) width at broadened segment, and (d) position at broadened segment.

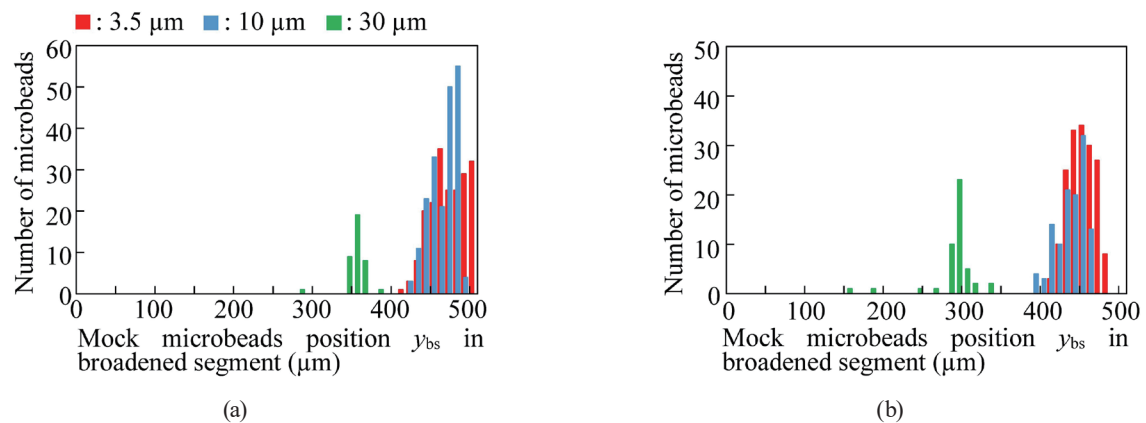


Fig. 4. (Color online) Effects of the pinched segment with mock microbeads separation performance in mock test: flow rate of (a) 1:10 and (b) 1:20.

($440.7 \pm 17.8 \mu\text{m}$), and $158.8\text{--}339.5 \mu\text{m}$ ($289.0 \pm 28.7 \mu\text{m}$), respectively [Fig. 4(b)]. The CVs of y_{bs} for 3.5, 10, and 30 μm mock microbeads were 3.6, 4.0, and 9.9%, respectively. The displacement of the mock microbeads was inversely proportional to their diameter regardless of the flow rate.

3.3 Separation of WBCs

Figure 5 shows the separation performance of the WBCs by the microchannel, measured by using the CCD camera. The range, mean \pm SD, and CV of the position y_{bs} were $366.0\text{--}469.3 \mu\text{m}$, $429.6 \pm 16.9 \mu\text{m}$, and 3.9%, respectively (Fig. 6).

Next, each particle including the WBCs was detected by using the WBC counting device (Fig. 7). The time widths of the detected signals for 3.5 and 10 μm mock beads, and WBCs were 4.0 and 14.6, and 12.6 ms, respectively. On the basis of flow velocity calculations, the time widths of the output signals at 4.0, 14.6, and 12.6 ms corresponded to diameters of 2.8, 10.2, and 10.5 μm , respectively, and these values were proportional to the particle diameter. The average time to reach $x = 1000 \mu\text{m}$ was $1.89 \pm 0.38 \text{ s}$ ($n = 10$) and thus the required time was negligible.

3.4 Counting of WBCs in raw bovine milk

The particles in the raw bovine milk were counted by using the fabricated WBC counting device. The average number and diameter of MFGs in the raw bovine milk were estimated to be $3\text{--}5 \mu\text{m}$ and $1.07 \times 10^6 / \mu\text{L}$, respectively, in agreement with values in previous reports.^(18–20) The average number of WBCs in the raw bovine milk was estimated to be $6.93 \times 10^3 \text{ cells/mL}$, which was within the range of normal WBC values for healthy dairy cattle without mastitis.^(16,17)

Figure 8 shows the calibration curve of the WBC counting device obtained using raw bovine milk. The number of signals, N (pulses/min), had a linear relationship with the concentration of WBCs, WBC (cell/ μL).

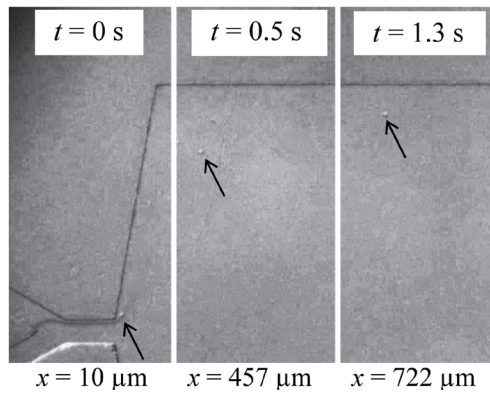


Fig. 5. Time-course changes of positions of WBCs after passing pinched segment (sample liquid:sheath liquid ratio = 1:10). Cells were indicated by arrows.

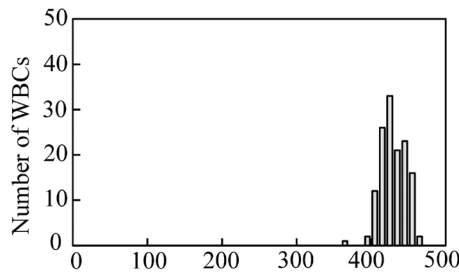


Fig. 6. Effect of the pinched segment on WBC separation performance ($n = 136$).

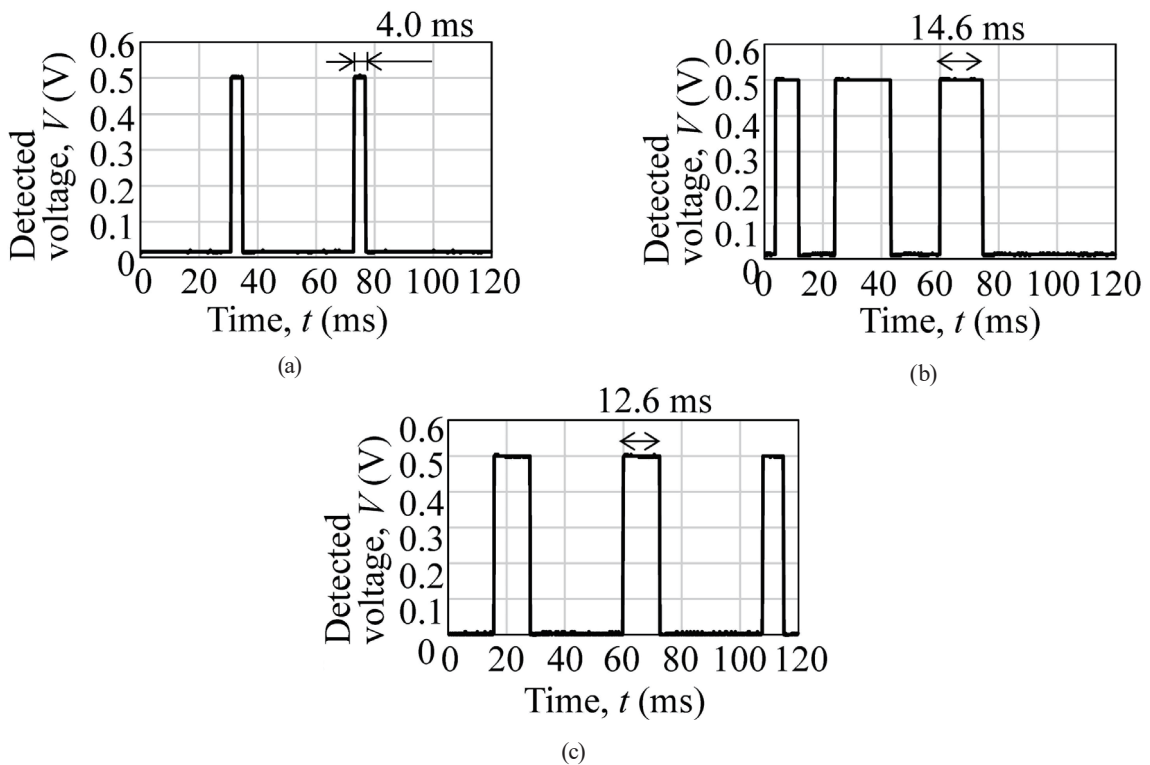


Fig. 7. Comparison of detected signals between mock microbeads and WBCs (4.0, 14.6, and 12.6 corresponding to diameters of 2.8, 10.2, and 10.5 μm , respectively): (a) 3.5 μm of resin particle, (b) 10 μm of resin particle, and (c) WBC.

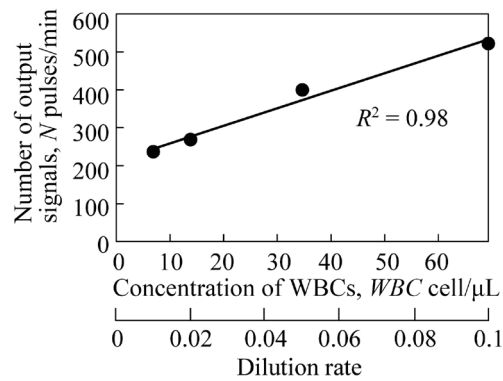


Fig. 8. Calibration curve of WBC counting device using raw bovine milk ($N = 6408.2 \text{ WBC} + 425.1$).

$$N = 6408.2 \text{ WBC} + 425.1 \text{ (pulses/min)}, \quad (1)$$

where the flow rate of the sample liquid was $0.2 \mu\text{L}/\text{min}$.

The linear regression analysis of the calibration curve for the WBC counting device showed a multiple determination coefficient, R^2 , of 0.98 for concentrations of WBCs between 6.9 and 69.3 cells/ μL .

4. Discussion

We designed the microchannel with the pinched and broadened segments used for the WBC counting device. From the results of the calculated streamlines (Fig. 3), the particle distribution was observed to approach the side wall of the pinched segment as the sheath flow rate increased. It was considered that the flow rate should be 1:10 or more. y_{bs} increased proportionally to the width of the broadened segment, l_{bs} ; however, it was estimated that it would be difficult to increase the difference in y_{bs} for 3.5 and 10 μm particles.

Firstly, the separation and counting characteristics of the WBC counting device were evaluated using mock microbeads. It has been reported that the diameters of WBCs and cancer cells were 10 and 30 μm , respectively.^(9,10) Therefore, the pinched flow microfluidic device based on FFF was useful for separating particles with diameters of 10 and 30 μm , and the flow rate of 1:10 was sufficient. However, it was difficult to separate particles with diameters of 3.5 and 10 μm , and these results agreed with our calculated results (Fig. 4).

Subsequently, the separation and counting characteristics of the WBC counting device were evaluated using WBCs. The position of the WBCs was consistent with the results for the 10 μm mock beads (Figs. 5 and 6). It was considered that measuring the time width of the output signal using light scattering could be an effective approach to separate particles with diameters of 3.5 and 10 μm passing through a close streamline (Fig. 7). The measuring time could be maintained within 1 min because counting 100 particles would be sufficient to calculate concentrations in field applications.

Finally, the counting of WBCs in raw bovine milk was performed. It was concluded that the counting of WBCs can be established from a calibration curve with $R^2 = 0.98$ for concentrations of WBCs between 6.9 and 69.3 cells/ μL using the WBC counting device (Fig. 8). A limitation to our study was that the detection signal included particles other than WBCs. The main causes of errors in detection could include the following: (1) sample causes: the agglutination of MFGs and (2) optical design causes: particles partially cross over the spot of the laser diode. To eliminate the errors due to the optical design, the spot diameter was set to approximately 100 μm , which was larger than the diameter of WBCs.

In future work, we intend to improve the discrimination ability by modifying the pretreatment conditions of samples by adding a surfactant and further optimizing the optical design.

5. Conclusions

The analytical performance of our particle counting device, using a microchannel incorporating light scattering, allowed the rapid measurement (<1 min) of the concentration of WBCs of dairy cattle, making it suitable for field applications. The performance characteristics of the WBC counting device were optimized using three different test samples including mock microbeads, WBCs, and raw bovine milk. The microfluidic device was able to separate particles with diameters above 10 μm . The incorporation of light scattering enabled the separation of particles with diameters of less than 10 μm passing through a close streamline, which were otherwise missed using the microchannel.

Acknowledgments

We would like to thank Professor Shinichi Yonekura, Laboratory of Animal Physiology, Department of Agriculture, Shinshu University, Japan, for his cooperation in providing raw bovine milk.

Funding

This research was supported in part by grant no. 20H04514 from the Japan Society for the Promotion of Science and was based on the ultrasensitive and rapid cancer testing technique based on fiber-type amplification (Principal Investigator: M. Yamaguchi).

Declaration of Competing Interest

The authors declare that they have no known competing financial interests or personal relationships that could have appeared to influence the work reported in this paper.

References

- 1 H. Zhang, C. H. Chon, X. Pan, and D. Li: *Microfluid. Nanofluid.* **7** (2009) 739. <https://doi.org/10.1007/s10404-009-0493-7>
- 2 Y. Zhang, J. Bai, H. Wu, and J. Y. Ying: *Biosens. Bioelectron.* **69** (2015) 121. <https://doi.org/10.1016/j.bios.2015.02.019>
- 3 T. Otto Mattsson, C. L. Lindhart, J. Schöley, L. Friis-Hansen, and J. Herrstedt: *Eur. J. Cancer Care (Engl)* **29** (2020) e13189. <https://doi.org/10.1111/ecc.13189>
- 4 J. W. Yarnell, I. A. Baker, P. M. Sweetnam, D. Bainton, J. R. O'Brien, P. J. Whitehead, and P. C. Elwood: *Circulation* **83** (1991) 836. <https://doi.org/10.1161/01.cir.83.3.836>
- 5 M. J. Green, L. E. Green, Y. H. Schukken, A. J. Bradley, E. J. Peeler, H. W. Barkema, Y. de Haas, V. J. Collis, and G. F. Medley: *J. Dairy Sci.* **87** (2004) 1256. [https://doi.org/10.3168/jds.S0022-0302\(04\)73276-2](https://doi.org/10.3168/jds.S0022-0302(04)73276-2)
- 6 S. Choi, S. Song, C. Choi, and J. K. Park: *Lab Chip* **7** (2007) 1532. <https://doi.org/10.1039/b705203k>
- 7 U. Emanuelson and H. Funke: *J. Dairy Sci.* **74** (1991) 2479. [https://doi.org/10.3168/jds.S0022-0302\(91\)78424-5](https://doi.org/10.3168/jds.S0022-0302(91)78424-5)
- 8 J. C. Giddings: *Separ. Sci.* **1** (1966) 123. <https://doi.org/10.1080/01496396608049439>
- 9 K. D. Caldwell, T. T. Nguyen, M. N. Myers, and J. C. Giddings: *Sep. Sci. Technol.* **14** (1979) 935. <https://doi.org/10.1080/01496397908058103>
- 10 M. E. Schimpf, K. Caldwell, and J. C. Giddings Eds.: *Field-flow Fractionation Handbook: The Field-flow Fractionation Family: Underlying Principles* (John Wiley & Sons, Inc. New York, 2000) pp. 3–30.
- 11 D. C. Duffy, J. C. McDonald, O. J. A. Schueller, and G. M. Whitesides: *Anal. Chem.* **70** (1998) 4974. <https://doi.org/10.1021/ac980656z>
- 12 L. R. Huang, E. C. Cox, R. H. Austin, and J. C. Sturm: *Science* **304** (2004) 987. <https://doi.org/10.1126/science.1094567>
- 13 M. Yamada, M. Nakashima, and M. Seki: *Anal. Chem.* **76** (2004) 5465. <https://doi.org/10.1021/ac049863r>
- 14 M. Yamada, K. Kano, Y. Tsuda, J. Kobayashi, M. Yamato, M. Seki, and T. Okano: *Microdevices* **9** (2007) 637. <https://doi.org/10.1007/s10544-007-9055-5>
- 15 H. Naito, Y. Ogawa, A. Kubota, and N. Kondo: *IFAC Proc.* **46** (2013) 331. <https://doi.org/10.3182/20130828-2-SF-3019.00040>
- 16 ISO13366-1/IDF148-1: *International Dairy Federation Standard* (2008) 1.
- 17 N. Li, R. Richoux, M. Boutinaud, P. Martin, and V. Gagnaire: *Dairy Sci. Technol.* **94** (2014) 517. <https://doi.org/10.1007/s13594-014-0176-3>
- 18 M. Martini, F. Salari, and I. Altomonte: *Crit. Rev. Food Sci. Nutr.* **56** (2016) 1209. <https://doi.org/10.1080/10408398.2012.758626>
- 19 A. Logan, M. Auld, J. Greenwood, and L. Day: *J. Dairy Sci.* **97** (2014) 4072. <https://doi.org/10.3168/jds.2014-8010>
- 20 L. Walter, S. Finch, B. Cullen, R. Fry, A. Logan, and B. J. Leury: *J. Dairy Res.* **86** (2019) 454. <https://doi.org/10.1017/S0022029919000748>
- 21 C. F. Bohren and D. R. Huffman: *Absorption and Scattering of Light by Small Particles* (John Wiley & Sons, Inc. New York, 1983) pp. 57–81.
- 22 S. A. Boothroyd, A. R. Jones, K. W. Nicholson, and R. Wood: *Combust. Flame.* **69** (1987) 235.
- 23 V. Kontturi, P. Turunen, J. Uozumi, and K. Peiponen: *Opt. Lett.* **34** (2009) 3743. <https://doi.org/10.1364/OL.34.003743>
- 24 J. Shi, F. Chen, Y. Cai, S. Fan, J. Cai, R. Chen, H. Kan, Y. Lu, and Z. Zhao: *PLOS ONE* **12** (2017) e0185700. <https://doi.org/10.1371/journal.pone.0185700>
- 25 W. Hashimoto, K. Takeda, R. Anzai, K. Ogasawara, H. Sakihara, K. Sugiura, S. Seki, and K. Kumaga: *J. Immunol.* **154** (1995) 4333.
- 26 A. Altmeyer and F. J. Dumont: *Cytokine* **5** (1993) 133. [https://doi.org/10.1016/1043-4666\(93\)90052-7](https://doi.org/10.1016/1043-4666(93)90052-7)
- 27 J. U. Brackbill, D. B. Kothe, and C. Zemach: *J. Comput. Phys.* **100** (1992) 335. [https://doi.org/10.1016/0021-9991\(92\)90240-Y](https://doi.org/10.1016/0021-9991(92)90240-Y)
- 28 S. E. Rogers and D. Kwak: *Am. Inst. Aeronaut. Astronaut. J.* **28** (1990) 253. <https://doi.org/10.2514/3.10382>
- 29 A. J. Chorin: *J. Comput. Phys.* **135** (1997) 118.